JOURNAL OF CATALYSIS 57, 458–475 (1979)

Adsorption and Temperature-Programmed Desorption of Hydrogen with Dispersed Platinum and Platinum–Gold Catalysts

J. R. ANDERSON,* K. FOGER, AND R. J. BREAKSPERE†

CSIRO Division of Materials Science, Catalysis and Surface Science Laboratory, University of Melbourne, Parkville, Victoria, Australia 3052

Received August 8, 1978; revised November 24, 1978

Hydrogen adsorption has been studied by temperature-programmed desorption (TPD) and by static volumetric measurement (SVM) on a range of supported dispersed platinum and platinum–gold catalysts. For compositions in the range Pt 98, Au 2 to Pt 15, Au 85 mole%, a comparison of hydrogen adsorption data with predictions from surface enrichment theory combined with electron microscopic particle size measurement, led to the conclusion that after suitable thermal treatment, equilibrium surface enrichment by gold was achieved, although equilibrium was most difficult to achieve for the Pt 15, Au 85 composition.

It was concluded from the nature of the hydrogen adsorption isotherms that, at higher pressures, some hydrogen could be adsorbed on surface gold atoms, probably as a result of spillover from the platinum component.

The general shape of the TPD profiles on platinum–gold was independent of gold content; to a first approximation the gold acted as an inert diluent. The implications of this result for the mode of hydrogen chemisorptive bonding are discussed.

With gold-free platinum catalysts there was a trend towards an extension of the high temperature tail of the TPD profile with decreasing $\bar{d}_{Pt}$ in the range $\leqslant 4$ nm, due to the presence of hydrogen binding states of higher energy. Possible reasons for this are discussed. Illustrations are given of the technique of TPD-profile dissection using increased starting temperatures. A TPD peak with a maximum in the region 700–750 K has been assigned to desorption from the support, this binding state being populated via hydrogen spillover from the platinum.

Temperature-programmed desorption has shown the existence of more than one binding state for hydrogen on platinum (*1–4*). There is some evidence that the relative population of the binding states varies with platinum dispersion (*2*) and with the component ratio in platinum–gold evaporated films (*3*). Furthermore, there is evidence that a particular binding state may be involved in a given catalytic reaction (*2, 5*).

Dispersed platinum is a catalyst of great importance, particularly for skeletal reactions of hydrocarbons (e.g., (*6*)), and more recently it has become clear that reactions of this type are strongly influenced by small (<10 at%) (*7*) as well as large (<85 at%) (*8, 37*) amounts of gold in platinum–gold catalysts.

If the metallic particles in a dispersed catalyst are sufficiently small, their intrinsic catalytic properties may be different from those of the massive metal, and the behavior of the metal may then be in-

* To whom correspondence should be addressed.
† On leave from University College, Cardiff, U. K.

0021-9517/79/060458-18$02.00/0

fluenced by the nature of the support: On the whole, effects of this sort appear to be found when the metallic particle diameter is less than about 2 nm (*9–12*). Additionally, with a dispersed alloy catalyst such as platinum–gold, there is the problem of understanding the catalytic activity in terms of composition: Much of this involves the way in which the concentration and reactivity of the relevant adsorbed species are controlled by the surface composition and by the arrangement of the component atoms in the surface.

In order to illuminate these problems, we have studied hydrogen adsorption and temperature-programmed desorption with a range of platinum and platinum–gold catalysts in which we have varied the metallic dispersion, the nature of the support, and the composition of the alloy phase.

EXPERIMENTAL

Temperature-Programmed Desorption

The apparatus follows the main features indicated in the design due to Aben *et al.* (*2*). Two alternative gas-composition detection systems were used, both involving thermal conductivity detection: (i) an Aerograph Model 1520 gas chromatograph, and (ii) a Carle Model 111H gas chromatograph. In the latter, a hydrogen-specific detection system is used, involving hydrogen transfer across a heated palladium thimble. Provided adequate gas purity was maintained, both detection systems gave similar results, although the latter system proved to be the more convenient and precise. The sensitivity for gas detection was determined by injection through a septum. In practice, great care needs to be exercised to avoid the generation of spurious TPD peaks due to the desorption of traces of moisture from the sample, and from the effects of variation in sweep gas flow rate consequent upon heating the sample.

For TPD, heating rates in the range 10 to 40 K min^{-1} were used, with sweep gas flow rates in the range 10 to 25 cm^3 min^{-1}. Bottled gases of the highest commercial grade of purity were used.

Gas Adsorption from Static Volumetric Measurement

Adsorption measurements were made using an all-glass volumetric adsorption apparatus of standard design. Samples were reduced in hydrogen at 620 K for 16 hr, outgassed to about 10^{-3} Pa at 520 K, and hydrogen adsorption measurements were made at 293 K. Hydrogen was purified by palladium diffusion. The method for estimating monolayer coverage is indicated in subsequent sections.

Catalyst Preparation

Platinum/silica gel. The support was a low area silica gel (80 m^2g^{-1}), crushed and sieved to 0.4 mm. The catalyst was prepared by impregnation with chloroplatinic acid solution using the method of incipient wetness, followed by drying with constant stirring to 370 K for 8 hr, calcining in flowing air at 620 K for 5 hr, and reduction in flowing hydrogen at 620 K. Nominal catalyst composition: 2 wt% platinum.

Platinum/aerosil. Two catalysts of this sort were prepared. High dispersion: prepared by adsorption of $Pt(NH_3)_4^{2+}$ onto aerosil as described by Moss *et al.* (*13*). After adsorption, the catalyst was washed, dried for 3 hr in air at 370 K, calcined in flowing oxygen at 573 K for 5 hr, and reduced in hydrogen at 620 K. Nominal catalyst composition: 2 wt% platinum. Low dispersion: Prepared as described above for platinum/silica gel. Nominal catalyst composition: 1 wt% platinum.

Platinum/(Na)Y-zeolite. This was prepared by exchanging $Pt(NH_3)_4^{2+}$ into (Na) Y-zeolite (Linde SK-40). After exchange and thorough washing, the product was dried at 370 K for 5 hr, followed by

TABLE 1

Data for Platinum Catalysts

Catalyst	Hydrogen adsorption[a] (10^{20} H_2/g Pt)		Platinum dispersion[c]	Average platinum particle diameter (nm)[d]	
Pt/silica gel, 2.0 wt% Pt	0.43	(0.40)[b]	0.03[b]	42	
Pt/aerosil					
low dispersion, 0.90 wt% Pt	4.11	(3.8)	0.26	4.1	(4.0 ± 0.3)
high dispersion, 1.95 wt% Pt	—	(15.4)	(1.0)	1.1	(1.3 ± 0.5)
Pt/(Na)Y-zeolite, 3.0 wt% Pt	15.8	(13.7)	1.05	1.0	(1.0 ± 0.5)
Pt/(La)Y-zeolite, 3.0 wt% Pt	16.0	(15.1)	1.05	1.0	(1.0 ± 0.5)
Pt/γ-alumina, 1.0 wt% Pt					
low dispersion		(5.2)	(0.35)	3.2	
high dispersion		(14.2)	(0.94)	1.2	

[a] At 293 K, "saturated" uptake.

[b] Bracketed figures by TPD, other figures by SVM.

[c] Based where possible on SVM data.

[d] Unbracketed figures from the platinum dispersion, bracketed figures from electron microscopy.

calcining in dry flowing oxygen at 620 K for 4 hr, following the procedure recommended by Dalla Betta and Boudart (*14*). Nominal catalyst composition 3 wt% platinum.

Platinum/(La)Y-zeolite. This was prepared by exchanging the residual Na^+ in the platinum/(Na)Y-zeolite with La^{3+}, using a solution of lanthanum nitrate. The lanthanum exchange was done after the platinum/(Na)Y-zeolite had been calcined and reduced. After exchange the catalyst was washed, dried at 370 K, and reduced again at 620 K. Nominal catalyst composition: 3 wt% platinum.

Platinum/γ-alumina. This was prepared by impregnation of γ-alumina (200 m^2g^{-1}) using the same method as described for platinum/silica gel. Nominal catalyst composition: 1 wt% platinum. Two catalysts were prepared. High dispersion: obtained after reduction in hydrogen at 620 K. Low dispersion: after heating in hydrogen at 920 K for 16 hr.

Platinum–gold/aerosil. The method of preparation followed that indicated above for platinum/aerosil, using coimpregnation with a solution containing chloroplatinic acid and chloroauric acid. Nominal catalyst composition: total metal 1 wt%.

Catalyst compositions were measured after preparation by X-ray fluorescence, and the data are included in Tables 1 and 2.

HYDROGEN ADSORPTION AND CATALYST CHARACTERIZATION

Hydrogen adsorption measurements were made both by static volumetric measurement (SVM) and by TPD. For this purpose TPD measurements were made using a sweep gas containing 0.1 vol% hydrogen in argon. Depending on the pressure of sweep gas over the sample, which in our experiments ranged 1 to 1.5 atm, the hydrogen pressure over the sample during equilibration before beginning a TPD run was about 0.10 to 0.15 kPa. The hydrogen uptake estimated by TPD includes everything under the TPD profile above 293 K but not including the contribution from a peak at about 740 K which is attributed to desorption from the zeolite (vide infra).

This high-temperature peak does not amount to more than 10 to 15% of the

TABLE 2

Data for Platinum–Gold Catalysts

Catalyst	Hydrogen adsorption[a] (10^{20} H_2/g metal)		Average metallic particle size by electron microscopy (nm)	Calculated equilibrium surface composition[b]	Calculated hydrogen adsorption (10^{20} H_2/g metal)
Pt–Au/aerosil					
1.0 wt% metal; Pt 98, Au 2[b]	3.49	(3.4)[c]	4.0 ± 0.3	Pt 92, Au 8	3.40
0.9 wt% metal; Pt 90, Au 10	2.18	(1.7)	4.0 ± 0.3	Pt 58, Au 42	2.14
0.9 wt% metal; Pt 76, Au 24	6.67		1.5 ± 0.2	Pt 65, Au 35	6.61
0.9 wt% metal; Pt 67, Au 33	4.00		1.7 ± 0.2	Pt 43, Au 57	4.20
1.0 wt% metal; Pt 15, Au 85					
"standard"[d]	1.60		2.0 ± 0.2	Pt < 1, Au > 99	<0.1
"equilibrated"	0.04		2.2 ± 0.2		

[a] At 293 K, "saturated" uptake.
[b] Component composition as mole%.
[c] Bracketed figures by TPD, other figures by SVM.
[d] Terms defined in text.

total, and this correction can be made without serious error.

Platinum Catalysts

The data for the platinum catalysts are contained in Table 1. Monolayer hydrogen uptakes were estimated by SVM in the usual way by back-extrapolation from the part of the isotherm linear in the range 1 to 7 kPa.

In addition to hydrogen adsorption data, Table 1 also lists values for the platinum dispersion and the average platinum particle diameter. The platinum dispersion, defined in the usual way as the ratio $N_{(S)Pt}/N_{(T)Pt}$, was calculated assuming a hydrogen monolayer chemisorption stoichiometry of two, that is two surface platinum atoms for every adsorbed molecule of hydrogen. Values for the average platinum particle diameter are listed both as calculated from the platinum dispersion on an equivalent spherical particle model, and from direct measurement by electron microscopy. The two methods for average platinum particle size estimation give results in good agreement which validates the model assumed for the hydrogen monolayer chemisorption stoichiometry, and is in agreement with previous data (cf. Ref. (*9*)).

Platinum–Gold Catalysts

With these catalysts there is the problem of alloy equilibration, and the conditions necessary to achieve this varied with alloy composition. With compositions in the range Pt 98, Au 2 to Pt 67, Au 33 mole%, initial preparation followed by two oxidation (oxygen, 573 K, 5 hr)/reduction (hydrogen, 620 K, 16 hr) cycles gave catalysts for which the hydrogen adsorption behavior did not change significantly either with further oxidation/reduction cycling or with extended periods of reduction in hydrogen at 620 K. This behavior, and an interpretation of the hydrogen uptake data in terms of surface composition (vide infra) indicate that with these catalysts, this treatment resulted in alloy equilibration.

On the other hand, with the composition Pt 15, Au 85, alloy equilibration (as judged from the criteria indicated above) was much more difficult to achieve. Hydrogen adsorption behavior was approximately

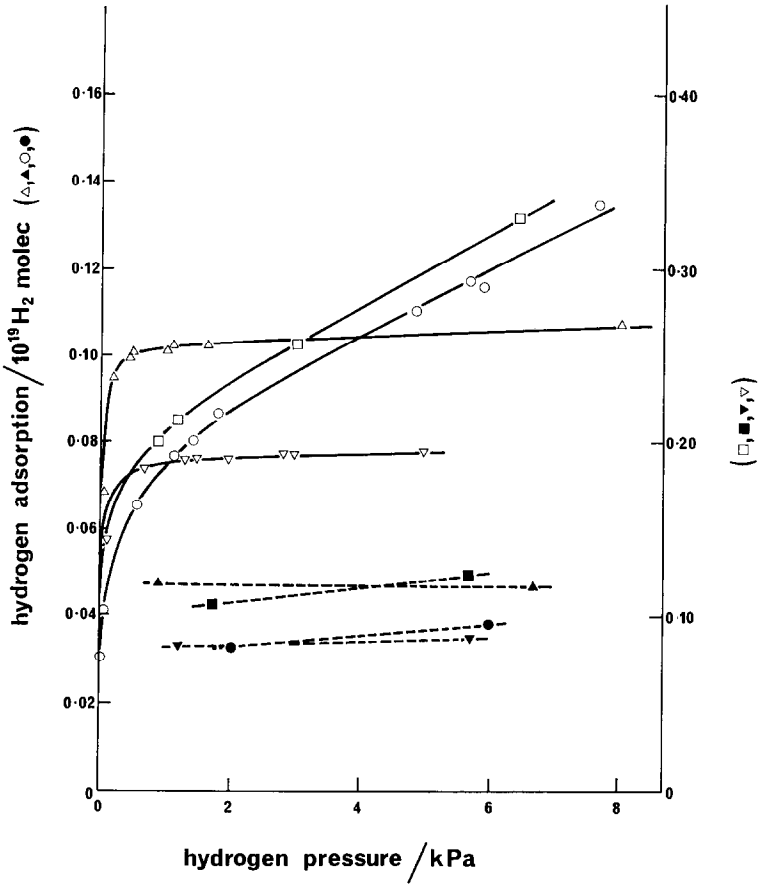

FIG. 1. Hydrogen adsorption isotherms at 293 K with platinum–gold/aerosil catalysts. ▽, Pt 98, Au 2 mole%, 1.0 wt% metal, 0.516 g catalyst; △, Pt 90, Au 10, mole%, 0.9 wt% metal, 0.510 g catalyst; □, Pt 67, Au 33 mole%, 0.9 wt% metal, 0.500 g catalyst; ○, Pt 15, Au 85 mole%, 1.0 wt% metal, 0.450 g catalyst; "standard" pretreatment (cf. text). Filled symbols, amount of adsorbed hydrogen remaining after pumping at 293 K for 30 min, after equilibration at indicated pressure. Catalyst samples identified from corresponding symbols above. Within the limits of experimental accuracy, no adsorption could be detected on a Pt0, Au 100 mole%, 1.0 wt% catalyst, using a 0.500-g sample.

independent of further oxidation/ reduction after about five cycles (involving > 100 hr at elevated temperatures). We refer to a catalyst of this composition having had this treatment as "equilibrated," and two oxidation/reduction cycles as "standard." The need for a number of oxidation/reduction cycles to achieve alloy equilibration was previously reported by O'Cinneide and Gault (*37*) for a Pt 15, Au 85/γ-alumina catalyst.

Hydrogen adsorption isotherms. The nature of the 293 K SVM hydrogen adsorption isotherms was dependent on the gold content of the catalysts, as is evident from the data shown in Fig. 1. Also included in Fig. 1 is an estimate for the amount of irreversibly adsorbed hydrogen which remains on the catalyst after pumping for 30 min at 293 K. This estimate was made by pumping after hydrogen equilibration, and then measuring the amount of hydro-

gen required to be adsorbed to recover the previously established point on the isotherm (identified in terms of the equilibrium pressure): the difference between the total and second uptake is equated to the irreversibly adsorbed hydrogen.

In general shape, the adsorption isotherms for the Pt 98, Au 2 and Pt 90, Au 10 catalysts were rather similar to those found for gold-free catalysts, with linear and nearly horizontal plots at p_{H_2} above about 1 kPa. However, for the Pt 67, Au 33 and Pt 15, Au 85 specimens, the hydrogen uptake continued to increase at pressures above 1 kPa, although in this range these isotherms were also approximately linear. Clearly, when the gold content of the metallic component was substantial, the hydrogen adsorption isotherm at 293 K did not saturate in the same way as it did with a catalyst of low (or zero) gold content. On the other hand, on all catalysts the size of the irreversibly adsorbed hydrogen component (as operationally defined above) was approximately independent of the hydrogen equilibration pressure.

Catalyst characterization. The interpretation of the hydrogen adsorption data on the platinum–gold catalysts requires knowledge about the nature of the metallic particles and their surface composition. Except for the two catalysts of compositions Pt 98, Au 2 and Pt 15, Au 85, the catalysts used in the present work lie in the two-phase region of the platinum–gold phase diagram (*15*) at the maximum temperature of catalyst treatment (ca. 600–700 K). Nevertheless, we could find no evidence for more than a single metallic phase by X-ray diffraction with those catalysts for which the average metallic particle size was large enough to make this examination feasible (4 nm). We therefore proceed on the basis of single-phase alloy particles, and we assume the surface composition to be dictated by equilibrium enrichment thermodynamics. The validity of the model is then assessed by comparing calculated and experimental hydrogen adsorption data.

Since the molar volumes of platinum and gold are very similar (9.10 and 10.20 cm^3, respectively), this factor will have a negligible effect on the free energy change for surface enrichment, and we have thus calculated the equilibrium surface composition using regular solution surface enrichment theory (*16*). We used the parameter values $\gamma_{Pt} - \gamma_{Au} = 0.67$ J m^{-2} (*17*), $T = 600$ K, the regular solution interchange energy 1.25 kJ mol^{-1} (*18*) per nearest neighbor interaction, assuming a (100) surface, and the average area per atom in the alloy surface 7.99×10^{-20} m^2. In computing surface compositions with small alloy particles, account must be taken of the depletion of the bulk which accompanies surface enrichment, by applying the necessary mass balance criteria. The resulting values for the calculated surface compositions (which depend on average particle size) are listed in Table 2.

Since we wish to use the hydrogen adsorption data to estimate the number of platinum atoms in the surface of the metallic component, it is necessary to obtain a criterion which defines a state with a known hydrogen chemisorption stoichiometry.

Since the procedure of back-extrapolation from the linear part of the adsorption isotherm is valid with supported platinum catalysts for estimating monolayer hydrogen uptake (*9*), we have also adopted this procedure with the platinum–gold catalysts, assuming that the hydrogen uptake so defined is equivalent to one hydrogen atom per surface platinum atom. The validity of this procedure will be justified a postiori. However, we note here that it assumes, in effect, that the upward slope of the linear parts of the isotherms for the Pt 67, Au 33 and Pt 15, Au 85 catalysts (cf. Fig. 1) results from weak adsorption over-and-above the above amount required to give the as-

sumed chemisorption stoichiometry, and that isolated surface platinum atoms can nevertheless become populated with chemisorbed hydrogen atoms (vide infra).

The experimental hydrogen uptakes evaluated in this way are recorded in Table 2, together with the calculated uptakes, obtained from the data for the computed surface compositions.

The agreement between the experimental and calculated hydrogen adsorption is reasonably good, and the model is clearly validated. It should be noted, however, that, at the composition Pt 15, Au 85, the catalyst prepared by the "standard" treatment was obviously not equilibrated with respect to surface composition, and at this composition equilibrium is relatively difficult to achieve.

TEMPERATURE-PROGRAMMED DESORPTION PROFILES

TPD Profiles for Platinum

The general nature of the TPD profiles (300–700 K) obtained from hydrogen adsorbed at 293 K on a range of platinum catalysts is shown in Fig. 2. The most conspicuous feature is the change in the nature of the profile with changing values for the average platinum particle diameter ($\bar{d}_{Pt}$). A comparison of curves 1 and 2 shows that when the platinum particles are relatively large (4.1–4.2 nm), changing $\bar{d}_{Pt}$ has little effect on the general profile shape. However, in the range 1.0 to 4.1 nm (curves 3–7) a decreased value for $\bar{d}_{Pt}$ is accompanied by a broadening of the profile, the main feature of which is an extension of the high temperature profile tail. This trend occurs with aerosil as well as γ-alumina supports, although the effect is somewhat greater with γ-alumina. Furthermore, γ-alumina and Y-zeolite appear to have about the same effect, although with Y-zeolite support the profiles also show evidence for some very poorly resolved subsidiary maxima which are not seen with γ-alumina. Curves 1 to 7 also show a modest trend for the temperature of the profile maximum (T_m) to shift to a higher temperature as $\bar{d}_{Pt}$ decreases.

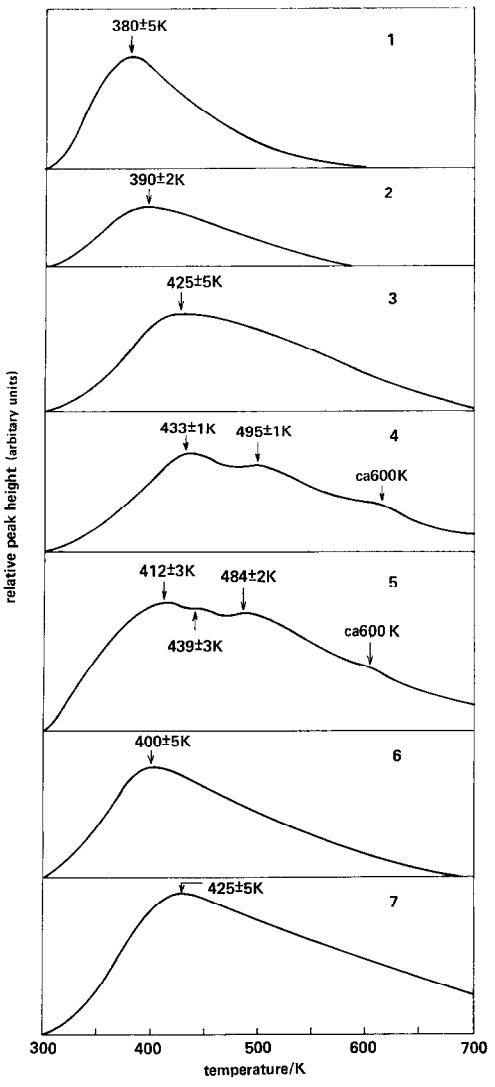

FIG. 2. TPD profiles for hydrogen from platinum catalysts. Curve 1, Pt/SiO_2-gel, $\bar{d}_{Pt}$ = 42 nm; curve 2, Pt/aerosil $\bar{d}_{Pt}$ = 4.1 nm; curve 3, Pt/aerosil, $\bar{d}_{Pt}$ = 1.2 nm; curve 4, Pt/(Na)Y-zeolite, $\bar{d}_{Pt}$ = 1.0 nm; curve 5, Pt/(La)Y-zeolite, $\bar{d}_{Pt}$ = 1.0 nm; curve 6, Pt/γ-Al_2O_3, $\bar{d}_{Pt}$ = 3.2 nm; curve 7, Pt/γ-Al_2O_3, $\bar{d}_{Pt}$ = 1.2 nm. Catalysts equilibrated in sweep gas at 293 K. Heating rate 20 K min^{-1}.

Changing the associated cation in platinum/Y-zeolite from Na^+ to La^{3+} had

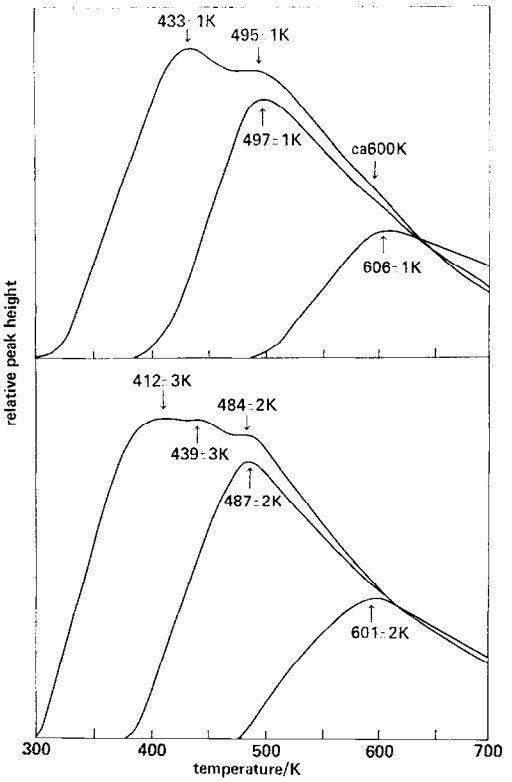

FIG. 3. TPD profiles for hydrogen from platinum/Y-zeolite catalysts with increasing starting temperatures. Curve 1, starting temperature 293 K; curve 2, 393 K; curve 3, 493 K. Catalysts equilibrated in sweep gas at indicated starting temperatures. Heating rate 20 K min^{-1}. Upper, platinum/(Na)Y-zeolite; lower, platinum/(La)Y-zeolite.

relatively small but significant effects on the profile: The two maxima which are present in the Na^+ sample at 433 and 495 K are replaced by three maxima of 412, 439, and 484 K (in all cases poorly resolved), and the whole profile is somewhat broadened with La^{3+}.

There are several reasons for believing that diffusional effects are, at the most, of minor importance in producing enhanced profile broadening. First, it was observed that a narrow pulse of hydrogen passed through samples of the (metal-free) supports (Y-zeolite, γ-alumina, or aerosil) was broadened to about the same extent in each case, and to an extent that was small compared to the profile widths. Second, we note that the variation in profile width with changing $\bar{d}_{Pt}$ occurred with all three supports and, in particular, occurred to about the same extent with γ-alumina as with Y-zeolite despite the large difference in surface area of these two supports. Third, we note that when the profile from platinum/Y-zeolite is dissected (cf. Fig. 5), the component peaks are nearly symmetrical, and this would not be so if diffusional limitation to gas transport in the support was a serious factor.

Blank TPD runs were carried out on samples of the platinum-free supports. In the range below 700 K only (La)Y-zeolite gave a significant peak, which was at 340 K. However, the area under this peak amounted to only about 1% of the area under the profile from the corresponding platinum-containing catalyst, and this contribution has, without loss of accuracy, been subtracted out of the recorded profiles which involve this support.

In the temperature range above 700 K, both (Na)Y- and (La)Y-zeolites gave desorption peaks which, although always smaller than those arising from the platinum-containing catalysts, are nevertheless appreciable. In this temperature range the situation is complicated by hydrogen spillover, and the results are discussed in more detail subsequently. There is no doubt that the above-700 K peaks were due to hydrogen since they were detected with the hydrogen-specific Carle IIIH unit.

Dissections of a profile may be made by carrying out the hydrogen adsorption equilibration and beginning the TPD run at a sequence of increasing temperatures. The effect of this procedure is to depopulate low energy binding states which would otherwise generate desorption peaks which overlap with a given peak on the low temperature side. Results obtained in this way with Pt/(Na)Y-zeolite and Pt/(La)Y-zeolite in the range 293 to 700 K are illustrated in Fig. 3. In principle, the choice

of starting temperatures for this sort of dissection is purely arbitrary, although with these two samples the values were selected by reference to the temperatures of the subsidiary maxima in the profile.

In addition to the binding states indicated by the T_m values given in Figs. 2 and 3, there was also evidence with the Pt/(Na)Y-zeolite and Pt/(La)Y-zeolite catalysts for further binding states with T_m in the region 700 to 750 K, as shown in Fig. 4. With both catalysts, a TPD profile starting at 293 K showed a relatively small but unmistakable T_m at about 740 K.

Increasing the starting temperature to 393 K had little effect, but at starting temperatures above 493 K the size of the peak in the region 700 to 750 K increased strongly. Inasmuch as the use of TPD routines with higher starting temperatures means that the sample was equilibrated for extended periods in hydrogen at high temperatures, the extent of these peaks appears to be mainly associated with

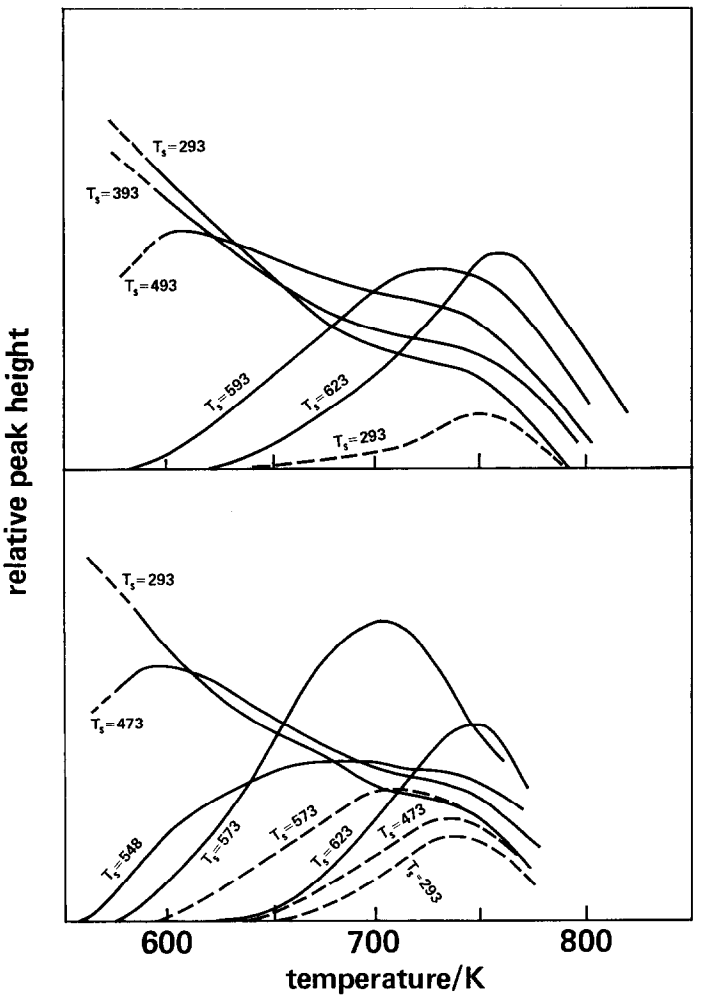

FIG. 4. TPD profiles >550 K for hydrogen from: upper, platinum/(Na)Y-zeolite; lower, platinum/(La)Y-zeolite. T_s values are for starting temperatures. Dotted curves are for platinum-free Y-zeolite. Catalysts equilibrated in sweep gas at indicated starting temperatures. Heating rate 20 K min^{-1}.

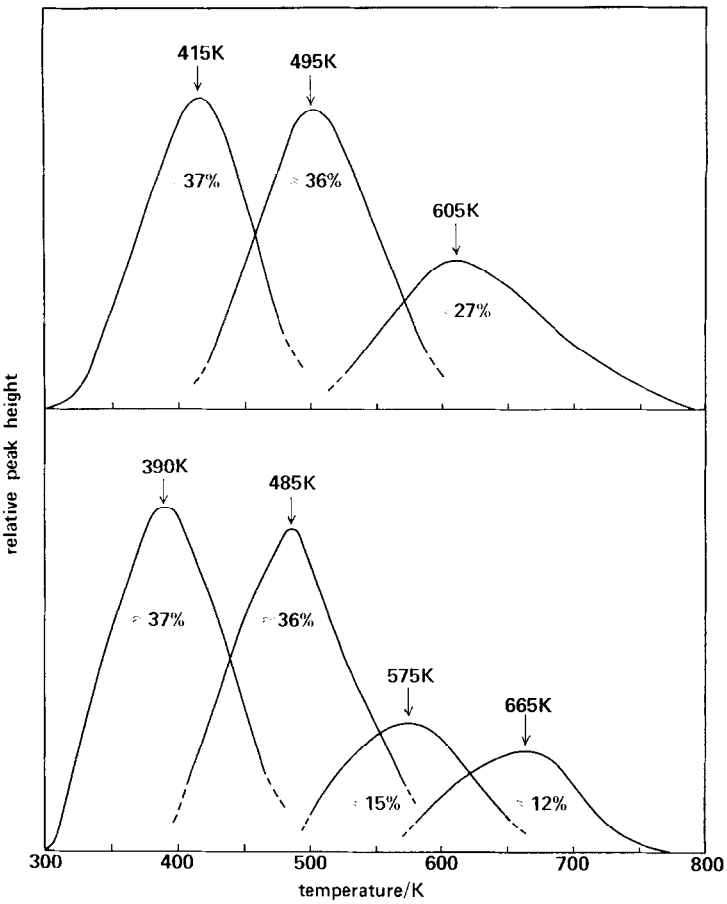

FIG. 5. Resolution of individual peaks which contribute to TPD profiles. Obtained by sequential curve subtraction from data in Figs. 3 and 4. Upper, platinum/(Na)Y-zeolite; lower, platinum/(La)Y-zeolite. Percentage figures indicate approximate peak contributions to total. Peaks attributed to desorption from zeolite have been eliminated.

hydrogen pretreatment of the catalyst at above about 500 K.

The curves for platinum-free zeolite in Fig. 4 show that zeolite itself gives a TPD peak in the 700 to 750 K region after treatment in hydrogen, but this is of itself insufficient to account for the size of the peaks obtained with the platinum-containing catalysts.

These peaks at 700 to 750 K are assigned to the desorption of hydrogen from the zeolite support, and this hydrogen consists of spillover hydrogen (that is, hydrogen first adsorbed on the platinum and transferred to the zeolite), together with some hydrogen intrinsically adsorbed on the zeolite (that is, adsorbed on the zeolite as in the absence of platinum). The reasons for this assignment may be summarized thus:

(i) The T_m values are closely similar in this temperature range for the platinum-containing and platinum-free materials;

(ii) the increased importance of these peaks with increasing extent of high temperature hydrogen treatment is consistent with this proposal;

(iii) the peaks cannot be due to dissolved hydrogen from the platinum since the

saturation solubility of hydrogen in platinum (about 1.5×10^{16} H_2 molec (g Pt)$^{-1}$ at 667 K) is too small to account for the magnitude of the peaks ($2-3 \times 10^{20}$ H_2 molec (g Pt)$^{-1}$; and

(iv) the peak position is close to that identified for spillover hydrogen with platinum/γ-alumina by Kramer (*22*).

The fact that on both catalysts referred to in Fig. 4 the profiles are essentially the same in the region of the maximum at 740 K irrespective of whether the starting temperature was 293 or 383 K suggests that under these conditions the 740 K maximum is due to hydrogen intrinsically adsorbed on the zeolite. Indeed, correction of the 293 K profiles for the intrinsically adsorbed hydrogen completely removes the 740 K peaks. This correction was made in order to obtain the TPD hydrogen adsorption estimates recorded in Table 1. On the other hand, the data in Fig. 4 show that, for catalysts treated in hydrogen above about 500 K, the spillover component must predominate in the hydrogen desorbed from the zeolite. With the peaks in the range 700 to 750 K assigned to desorption from the support, we assign all of the rest of the profile to desorption from platinum.

A partial resolution of some individual peaks which contribute to the total TPD profile is possible by making use of the dissections given in Figs. 3 and 4. A process of sequential curve subtraction, starting at the high temperature end, gives the results shown in Fig. 5 after elimination of the contribution attributed to desorption from the support.

Because peak overlap is extensive, the individual peak curves cannot be obtained with high accuracy. Nevertheless, an estimate of the individual peak contributions to the overall profile has been made from the peak areas, and these data are also given in Fig. 5. The proportional contributions of corresponding peaks for the two catalysts in Fig. 5 are in fair agreement. The T_m which was weakly indicated at 439 K in the 293 K profile from Pt/(La)Y-zeolite has not been resolved by this procedure, but has been lost into the trailing and leading edges of the 390 K and 485 K peaks.

TPD Profiles for Platinum–Gold

Figure 6 shows typical TPD profiles for platinum–gold/aerosil catalysts of varying gold content, obtained at a heating rate of 20 K min^{-1}. The important feature is that the general profile shape is independent of gold content, at least up to 85 mole% gold, and the value of T_m remained constant at about 390 K. No evidence of hydrogen adsorption could be obtained with a catalyst containing 100 mole% gold: The TPD profile is flat at 300 to 600 K.

DISCUSSION

Platinum Catalysts

On the whole, the estimates for hydrogen adsorption from TPD lie somewhat below those from SVM (*cf.* Table 1), and this is attributable to the lower hydrogen equilibration pressures used with the TPD method. Nevertheless, this comparison is sufficient to demonstrate that the TPD technique recovered all of the adsorbed hydrogen, and estimated it with adequate accuracy.

The trend towards an extension of the high temperature tail of the TPD profile with decreasing $\bar{d}_{Pt}$ in the range $\leqslant 4.1$ nm must be due to the presence of higher energy binding sites for hydrogen. In understanding this behavior, the following factors need to be considered. As the platinum particle size decreases, the proportion of surface platinum atoms of relatively low coordination number increases (corner atoms, kink atoms, atoms in high-index facets due to surface curvature). Furthermore, when $\bar{d}_{Pt}$ is sufficiently small, typically less than about 2 nm, there is evidence that the platinum behaves as

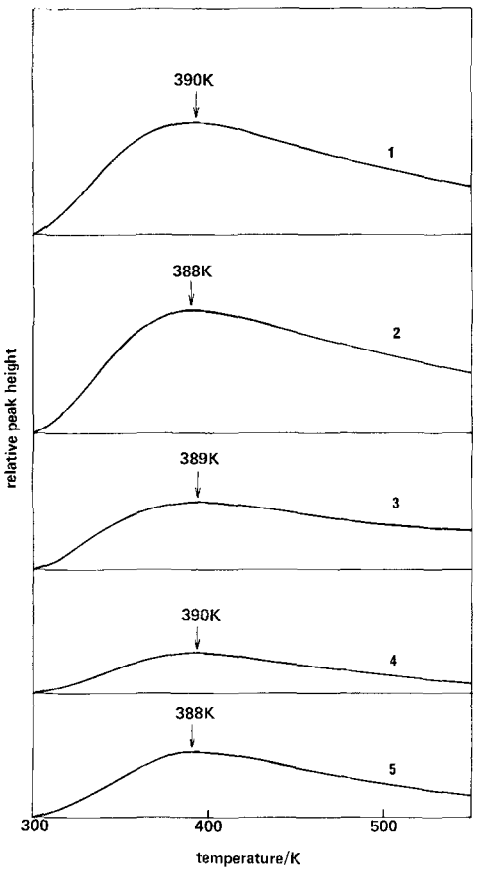

FIG. 6. TPD profiles for hydrogen from Pt/aerosil and Pt–Au/aerosil catalysts. Catalysts equilibrated in sweep gas at 293 K. Curve 1, Pt 100 mole%; curve 2, Pt 98, Au 2; curve 3, Pt 90, Au 10; curve 4, Pt 40, Au 60; curve 5, Pt 15, Au 85. Heating rate 20 K min^{-1}.

though it were electron deficient compared to bulk platinum. This is more evident with Y-zeolite support (*5, 14, 23*) than with silica support (*23*), but at the moment it is not clear if this difference is due to the platinum being more highly dispersed on the Y-zeolite than on the silica. In any case, the data are in agreement with the calculations for electron transfer between platinum and silica by Baetzold (*24*). We also note that even on bulk platinum, corner atoms are relatively electron deficient (*25, 26*).

These results may be understood in the light of the following considerations.

Calculations of the binding energy for chemisorbed hydrogen atoms show that particularly strong adsorption sites are provided at an edge in a stepped surface (*27*) or, to an even greater extent, at a kink atom of low coordination number (*28*). This implies that an atomically rough surface (as distinct from a low-index facet) will also possess a proportion of particularly strong adsorption sites.

Recent work (*28*) also shows that a chemisorbed hydrogen atom may well be bound more strongly at a platinum atom that is relatively electron deficient. In this connection, we first note that electrons close to the Fermi level are more likely to occupy antibonding orbitals than are electrons rather deeper in the valence band. Since electron deficient platinum would be generated by the removal of electrons at the Fermi level, this would offer an increase in the binding energy for hydrogen. In the detailed treatment by Tsang and Falicov (*28*), it was shown that the binding energy for hydrogen on platinum was always greater for $Pt^{2+}(5d^8)$ than for $Pt^{+}(5d^9)$ provided the coordination number of the platinum lay in the range 7 to 10.

Platinum–Gold Catalysts

We first consider our results for bulk-surface equilibration in comparison to other work on the platinum–gold system. In summary, our results indicate the establishment of equilibrium at all compositions, although at Pt 15, Au 85 equilibration was quite difficult to achieve.

Biloen *et al.* (*19*) have reported from Auger analysis and carbon monoxide chemisorption data that a clean platinum–gold polycrystal of bulk composition Pt 14, Au 86 gave, after treatment at 820 K, a surface composition in the range 5 to 10 mole% platinum; that is to say, very little surface enrichment by gold was found.

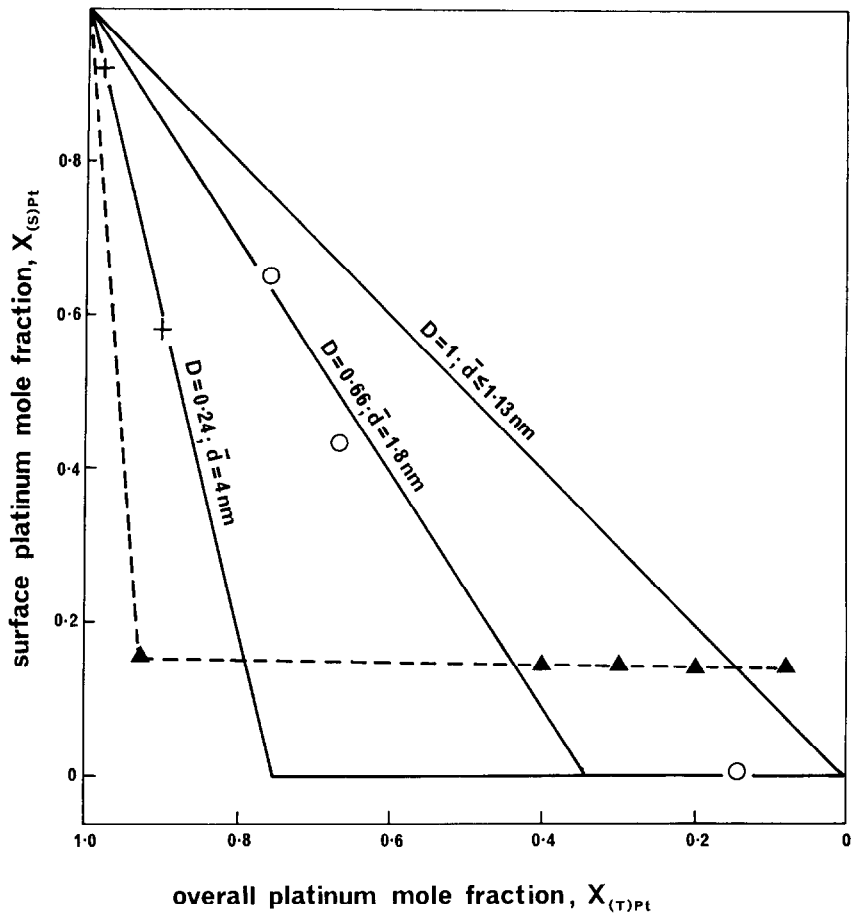

FIG. 7. Relative surface composition as a function of nominal alloy composition for various platinum–gold catalysts. Full lines calculated from model discussed in the text. Points are appropriate experimental values obtained from hydrogen adsorption data. ▲, evaporated platinum–gold films, cf. Ref. (*36*); +, platinum–gold/aerosil, $\bar{d}_{Pt}$ = 4.0 nm; ○, platinum–gold/aerosil, $\bar{d}_{Pt}$ = 1.5–2.2 nm.

On the other hand, Avery and Spink (*38*) used Auger analysis to study the surface composition of a clean Pt 10, Au 90 polycrystal, and found after treatment at 700 K very considerable surface enrichment by gold, a result that is in agreement with an earlier study by Schwarz *et al.* (*20*).

The present data may be compared with those obtained by Sachtler *et al.* (*36*) for hydrogen adsorption on platinum–gold evaporated films which showed a very rapid decrease in the amount of adsorbed hydrogen, and inferentially a corresponding decrease in the concentration of surface platinum atoms, in the range $\leqslant$7.5 mole% gold. This comparison is made in Fig. 7 which has been constructed in a way which shows the importance of the metallic dispersion (ratio of number of surface atoms to total number of atoms) as a variable.

Figure 7 was constructed in the following way. With a dispersed, binary alloy catalyst where there is strong segregation of one component at the surface, at segregation equilibrium it will be a good approximation to assume that, as the overall proportion

of the segregating component increases, it will be located entirely at the surface until all of the surface is occupied. Thus, on this model, a plot of overall alloy composition vs surface composition will consist of a family of lines, each for a particular dispersion: If the compositions are expressed in terms of the nonsegregating component (platinum in the case of platinum–gold, as in Fig. 7), that is $X_{(S)Pt}$ and $X_{(T)Pt}$ for the surface and overall platinum mole fractions respectively, each line will reach the $X_{(S)Pt} = 0$ line at a value of $X_{(T)Pt} = 1 - D$, where D is the metallic dispersion, and will continue along the $X_{(S)Pt} = 0$ line out to the point $X_{(T)Pt} = 0$.

The present experimental values for $X_{(S)Pt}$ vs $X_{(T)Pt}$ have been collected into Fig. 7, where $X_{(S)Pt}$ has been obtained from the hydrogen adsorption data as indicated previously. We also include in Fig. 7 the theoretical lines, obtained as outlined above, corresponding to the experimental metallic dispersions (for data from catalysts with $\bar{d}$ in the range 1.5 to 2.2 nm, we have used a single line at $D = 0.66$, corresponding to an average value of $\bar{d}$ of 1.8 nm). It is clear that this simple graphical representation is in good accord with the data.

For comparison, we also include in Fig. 7 the data obtained (*36*) from evaporated films. The effective dispersion of these films is not known, although the values are certain to be low compared with our dispersed catalysts. The rapid fall in $X_{(S)Pt}$ at low values of $X_{(T)Pt}$ is clearly in qualitative agreement with expectation, but the value $X_{(S)Pt} \approx 0.15$ for $0.925 > X_{(T)Pt} > 0.075$ probably indicates incomplete bulk–surface equilibration, particularly since those films were heated to 570 K for only about 3 hr.

At least so far as the dispersed catalysts are concerned, the achievement of surface segregation equilibrium under our conditions is consistent with data for diffusion kinetics. For instance, data (*21*) for interdiffusion in the platinum–gold system lead to estimates of interdiffusion distances of 43 and 3.1 nm at 673 and 573 K, respectively in a period of 1 hr.

Our results (cf. Table 2) show that the conditions required for the correct estimation of the number of surface platinum atoms in the platinum–gold system by hydrogen chemisorption are considerably different from those previously recommended with the nickel–copper system for the estimation of the number of surface nickel atoms (*29*). Thus, with nickel–copper the appropriate hydrogen adsorption is the "strong" adsorption component as operationally defined in relation to Fig. 1. However, it is clear that the application of a similar criterion to the platinum–gold system would underestimate the number of surface platinum atoms by at least a factor of two.

It seems clear that extrapolation from the behavior of one Group VIII–Group IB system to another is very hazardous, and hydrogen adsorption must be examined on each system in detail. The results imply that at high coverage, hydrogen is bound more strongly at the surface of nickel–copper than at platinum–gold.

That the general shape and T_m values for a number of TPD profiles are nearly constant for gold contents in the range 0 to 85 mole% (*cf.* Fig. 6), shows that alloying in the platinum–gold system does not greatly affect the distribution of hydrogen binding states as regards binding energy. With increasing gold content the TPD profile shrinks in an approximately uniform manner, and the system behaves as though gold atoms in the surface functioned only as inert diluent. An analogous conclusion has also recently been reached from flash desorption experiments with platinum–gold (*20*) and nickel–copper (*30*) foils.

We thus arrive at the conclusion that, so far as hydrogen chemisorption is con-

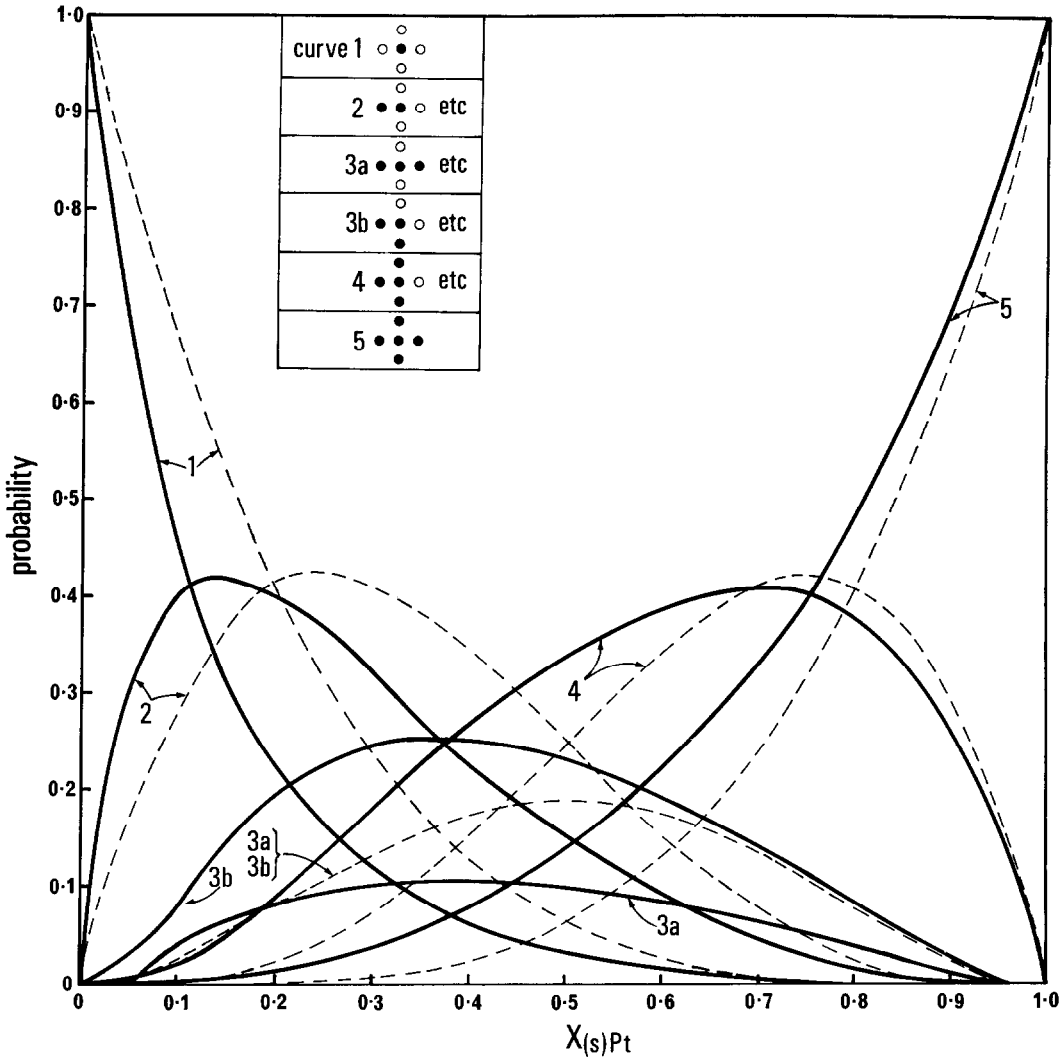

FIG. 8. Calculated distribution of surface ensembles in (100) platinum–gold surface. Full lines, using $\omega = 1.25$ kJ mol^{-1}. Broken lines, using $\omega = 0$ (random mixing). The probabilities are defined so that, given a surface platinum atom (●), the value is the chance of that atom having zero to four nearest neighbor platinum atoms.

cerned, the Group VIII metal orbitals which are used for chemisorption are largely unaffected by alloying with a Group IB metal. This may be rationalized in terms of a model recently adopted for bonding at transition metal surfaces (*32*) in which the *d* electrons are largely responsible for chemisorptive bonding and remain localized on the transition metal atoms. The metallic orbitals are mainly formed from atomic *s* and *p* orbitals. Recent calculations (*31*) have confirmed that hydrogen chemisorption on platinum and tungsten is determined almost entirely by the *d* electrons.

Our results indicate that all surface platinum atoms in a platinum–gold surface are available for hydrogen chemisorption, even though some of these may be isolated platinum atoms, that is to say, with no

nearest neighbor surface platinum atoms. We propose that isolated surface platinum atoms become populated with chemisorbed hydrogen atoms via hydrogen atom spillover onto the gold component in the surface. Such spillover may function in two possible ways: It may permit the transfer of hydrogen atoms to isolated platinum atoms from larger platinum ensembles where initial adsorption occurs, and/or a hydrogen molecule may be directly adsorbed at an isolated platinum atom provided one hydrogen atom becomes chemisorbed at an adjacent gold atom. We merely note that the binding of hydrogen atoms at a gold surface is well known (*34*) provided that the hydrogen is presented to gold in an atomic form. Rather analogous suggestions for spillover have previously been made for the nickel–copper system (*35*).

We further suggest that hydrogen spillover onto the gold is responsible for the "supra-saturation" hydrogen uptake which was particularly apparent with the Pt 67, Au 33 and Pt 15, Au 85 specimens (cf. Fig. 1). Clearly, such spillover would be reversible via adsorption/desorption at the platinum: That is to say, no hydrogen would be present on the gold under the conditions used to estimate saturated uptake on the platinum component.

Although with platinum–gold catalysts of various compositions the saturation concentration (as operationally defined previously) of adsorbed hydrogen per unit *total* area of metal varied, there was no evidence that this variation affected the value of T_m, despite the expectation of such a variation if the total surface had been active for the desorption process. This result is consistent with the idea that platinum–gold surfaces with saturation hydrogen uptake behaved in TPD as though the uptake was defined relative only to the active component (platinum); that is to say, at saturation hydrogen uptake the TPD behavior was as though the initial surface concentration of hydrogen was constant and independent of gold content.

Distribution of Surface Ensembles

The atoms in an alloy surface will, even though the alloy is monophasic, exist in ensembles which are distributed according to size. This information is important for the catalytic properties of the alloy, while it is also of interest in relation to chemisorption behavior (e.g., the proportion of isolated platinum atoms in a platinum–gold surface).

The distribution of surface ensembles of platinum has been evaluated for the platinum–gold system by a computer simulation method which minimizes the energy of the two-dimensional array of specified overall composition and specified interchange energy, ω, (i.e., a solution of the Ising model for specified parameters). The computational technique is due to Verhagen and Harding (*31*). The following conditions were used: surface, (100); ω = 1.25 kJ mole^{-1} (*18*), T = 600 K, where ω is the regular solution interchange energy per nearest neighbor interaction.

The results are given in Fig. 8 which also indicates the nature of the ensembles considered. Figure 8 also gives, for comparison, the corresponding results obtained with $\omega = 0$, that is, for random mixing. As would be expected for platinum–gold (which is a segregating system), the use of a finite and realistic value for ω results, at all compositions, in a decrease in the proportion of isolated platinum atoms and an increase in the proportion of 5-atom ensembles, relative to the random mixing values. The behavior of ensembles of intermediate size is complicated, and whether the use of a finite value for ω increases or decreases the ensemble fraction depends on composition. The effect can

be nontrivial. For instance, at a bulk composition of 10 mole% platinum, the fraction of isolated platinum atoms calculated for $\omega = 1.25$ kJ mol^{-1} is 0.46, compared with 0.67 for the random mixing model.

ACKNOWLEDGMENTS

The authors are grateful for skilled assistance from Dr. J. V. Sanders with electron microscopy, and for help by Mr. R. G. Sherwood and Mr. M. R. Jestrimski with adsorption and TPD measurements. The authors are particularly grateful to Dr. A. M. Verhagen and Mr. M. Harding for making their computer simulation technique available before publication, and for essential help with its application to the platinum-gold system. Finally (but not least) we are grateful to Professor H. Gruber for illuminating discussions concerning hydrogen spillover phenomena.

REFERENCES

1. Tsuchiya, S., Amenomiya, Y., and Cvetanovic, R. J., *J. Catal.* **19**, 245 (1970).
2. Aben, P. C., van der Eijk, H., and Oelderik, J. M., *in* "Proceedings, 5th International Congress on Catalysis" (J. W. Hightower, Ed.), p. 717. North-Holland, Amsterdam, 1973.
3. Stephan, J. J., Ponec, V., and Sachtler, W. M. H., *Surface Sci.* **47**, 403 (1975).
4. Möger, D., Besenyei, G., and Nagy, F. *React. Kinet. Catal. Lett.* **3**, 231 (1975).
5. Foger, K., and Anderson, J. R., *J. Catal.* **54**, 318 (1978).
6. Anderson, J. R., *Advan. Catal.* **23**, 1 (1973); Sinfelt, J. H., *Advan. Catal.* **23**, 91 (1973).
7. Anderson, J. R., and Foger, K., unpublished work from this laboratory.
8. Dessing, R. P., and Ponec, V., *Reaction Kinet. Catal. Lett.* **5**, 251 (1976); Dessing, R. P., and Ponec, V., *J. Catal.* **44**, 494 (1976).
9. Anderson, J. R. "Structure of Metallic Catalysts." Academic Press, London/New York, 1975.
10. Rabo, J. A., Schomaker, V., and Pickert, P. E., *in* "Proceedings, 3rd International Congress on Catalysis" (W. M. H. Sachtler, G. C. A. Schmit, and P. Zwietering, Eds.), p. 1264. North-Holland, Amsterdam, 1965.
11. Pickert, P., Rabo, J. A., Dempsey, E., and Schomaker, V., *in* "Proceedings, Third International Congress on Catalysis" (W. M. H. Sachtler, G. C. A. Schmit, and P. Zwietering, Eds.), p. 714. North-Holland, Amsterdam, 1965.
12. Rabo, J. A., Angell, C. L., Kasai, P. H., and Schomaker, V. *Discuss. Faraday Soc.* **41**, 328 (1966).
13. Dorling, J. A., Lynch, B. W. J., and Moss, R. L. *J. Catal.* **20**, 190 (1971).
14. Dalla Betta, R. A., and Boudart, M., *in* "Proceedings, 5th International Congress on Catalysis" (J. W. Hightower, Ed.), p. 1329. North-Holland, Amsterdam, 1973.
15. Hansen, M., "Constitution of Binary Alloys." McGraw-Hill, New York, 1958. Elliot, R. P., "Constitution of Binary Alloys," First Supplement. McGraw-Hill, New York, 1965.
16. van Santen, R. A., and Boersma, M. A. M., *J. Catal.* **34**, 13 (1974).
17. Overbury, S. H., Bertrand, P. A., and Somorjai, G. A., *Chem. Rev.* **75**, 547 (1975).
18. Jones, R. W., Stafford, F. E., and Whitmore, D. H., *Met. Trans.* 1, 403 (1970).
19. Biloen, P., Bouwman, R., van Santen, R. A., and Brongersma, H. H., *in* "Proceedings, 7th International Vacuum Congress, and 3rd International Conference on Solid Surfaces, 1977," Vol. 2, p. 1401.
20. Schwarz, J. A., Polizzotti, R. S., and Burton, J. J., *J. Vac. Sci. Technol.* **14**, 457 (1977).
21. Kincera, J., Fiedler, R., and Ciha, K., *Cesk. Casopis. Fys.* **A17**, 262 (1967).
22. Kramer, R. *J. Catal.*, in press.
23. Vedrine, J. C., Dufaux, M., Naccache, C., and Imelik, B., *in* "Proceedings 7th International Vacuum Congress, and 3rd International Conference on Solid Surfaces, 1977" Vol. 1, p. 481.
24. Baetzold, R. C., *J. Phys. Chem.* **80**, 1504 (1976).
25. Besocke, K., Kral-Urban, B., and Wagner, H., *Surface Sci.* **68**, 39 (1977).
26. Tsang, Y. W., and Falicov, L. M., *J. Phys. C.: Solid State Phys.* **9**, 51 (1976).
27. Fassaert, D. J. M., and van der Avoird, A., *Surface Sci.* **55**, 313 (1976).
28. Tsang, Y. W., and Falicov, L. M., *J. Molec. Catal.* **3**, 351 (1977/1978).
29. Sinfelt, J. H., Carter, J. L., and Yates, D. J. C., *J. Catal.* **24**, 283 (1972).
30. Yu, K. Y., Ling, D. T., and Spicer, W. E., *J. Catal.* **44**, 373 (1976).

31. Verhagen, A. M., and Harding, M. *J. Comput. Phys.*, in press.
32. Melius, C. F., *Chem. Phys. Lett.* **39**, 287 (1976).
33. Culver, R. V., Pritchard, J., and Tompkins, F. C., *Z. Elektrochem.* **63**, 741 (1959); Pritchard, J., and Tompkins, F. C., *Trans. Faraday Soc.* **56**, 540 (1960); Culver, R. V., Pritchard, J., and Tompkins, F. C., *in* "Proceedings, 2nd International Congress Surface Activity, 1957," Vol. 2, p. 243.
34. Campbell, J. S., and Emmett, P. H., *J. Catal.* **7**, 257 (1967).
35. Horiuti, J., and Toya, T., *Solid State Surface Sci.* **1**, 1 (1969).
36. Kuijers, F. J., Dessing, R. P., and Sachtler, W. M. H., *J. Catal.* **33**, 316 (1974).
37. O'Cinneide, A., and Gault, F. G., *J. Catal.* **37**, 311 (1975).
38. Avery, N. R., and Spink, J. V., unpublished work from this laboratory.